Comparison of Islanding and Synchronization for a Microgrid with Different Converter Control

Abdulhakim Alsaif
Department of Electrical Engineering
University of South Florida
Tampa, FL 33620, USA
IMBS University, Riyadh, KSA
alsaif1@mail.usf.edu

Zhixin Miao
Smart Grid Power Systems Lab
Department of Electrical Engineering
University of South Florida
Tampa, FL 33620, USA
zmiao@usf.edu

Lingling Fan
Smart Grid Power Systems Lab
Department of Electrical Engineering
University of South Florida
Tampa, FL 33620, USA
linglingfan@usf.edu

***Abstract*—This paper presents a comparison of microgrid performance during islanding and synchronization when different voltage source converter (VSC) controls are adopted. An overview of VSC controls, namely grid-following, grid-forming, and grid-supporting, is first provided. Comparison of microgrid performance is then conducted in two tesbeds built in MATLAB/SimPowerSystem environment. In the first testbed, a VSC switches back and forth between grid-following and grid-forming control during islanding and synchronization. An islanding scheme and a grid-back detection scheme are designed to automatically switch the operation modes of the VSC. In the second testbed, a VSC works in grid-supporting mode regardless of the microgrid operation mode. The two testbeds are compared side by side for their dynamic performance.**

***Index Terms*—Voltage source converter (VSC); grid-following; grid-forming; grid-supporting; islanding; synchronization.**

I. Introduction

MICROGRIDS (MGs) have the capability to operate either as grid-connected components or as islanded systems [1]. In grid-connected mode, frequency is regulated by the main grid. In islanded mode, voltage and frequency of a MG are regulated by itself [2], [3].

Voltage source converters (VSCs), which are the most common converters implemented in the modern grids, are the major components for interfacing distributed energy resources (DERs) to the main grid. Their control plays a significant role for stable and efficient performance in MGs [4]. The control structure of VSCs can be designed in different forms depending on the operation mode of the MG.

The three types of VSC controls are grid-following, grid-forming, and grid-supporting. A grid-following VSC regulates real and reactive power output of a VSC yet does not provide frequency support. A grid-forming VSC can provide both voltage and frequency control. With a grid-forming VSC, a MG can operate in islanded mode. Switching MGs'operation mode from one to another may require change of the control configuration of the converters. On the other hand, grid-supporting VSCs may operate for both grid-connected and islanded operation [2], [5]. This paper caries out a comparison study of the operation of these VSCs during MG islanding and synchronization.

978-1-7281-0407-2/19/$31.00 ©2019 IEEE

The paper is organized as follows. Section II presents a theoretical overview about different control configurations of VSCs in MGs. Section III presents the control design principal for each VSC control. Section IV describes the two simulation testbeds and the islanding and synchronization detection schemes. Section V presents the simulation results of two testbeds built in MATLAB/SimpowerSystem. Section VI concludes the paper.

II. Three types of VSC control

On the basis of VSC's operation modes in MGs (grid-connected or autonomous), it can be categorized into three types: grid-following, grid-forming, and grid-supporting [2].

A. Grid-Following VSC

The grid-following or grid-feeding VSC, is the vast majority converters implemented in renewable energy (e.g., solar PV and wind) grid integration [6]. It is primarily designed to exchange active and reactive power with an ac grid. Conventionally, a VSC is designed as a current source [7]. This design convention is also considered in this paper. At islanded operation, a MG requires a generator or a grid-forming converter to form the grid voltage and frequency [2].

In the dq-frame that is aligned to the voltage of the point of common coupling (PCC), the active and reactive power from the VSC can be controlled by the dq-axis currents, respectively [7]. This control is termed as vector control. Fig. 1 presents a typical control scheme for a grid-following VSC with two cascaded controllers based on the PCC voltage oriented dq-frame. The inner loop represents the converter current control. The reference current i_d^* can be created by regulating the outer loop of the active power at the PCC or the dc side link voltage control (gray lines). The reference current i_q^* can be generated by the reactive power control (gray lines), or by ac voltage control.

A synchronization mechanism is required in grid-following VSC in order to be synchronized with the grid. A phase-locked-loop (PLL) serves the purpose. A PLL extracts the grid frequency and PCC voltage angle θ_{pll}. It also ensures that the d-axis is aligned with the PCC voltage. In turn, the PCC voltage's q-axis component is forced to be zero [5], [8].

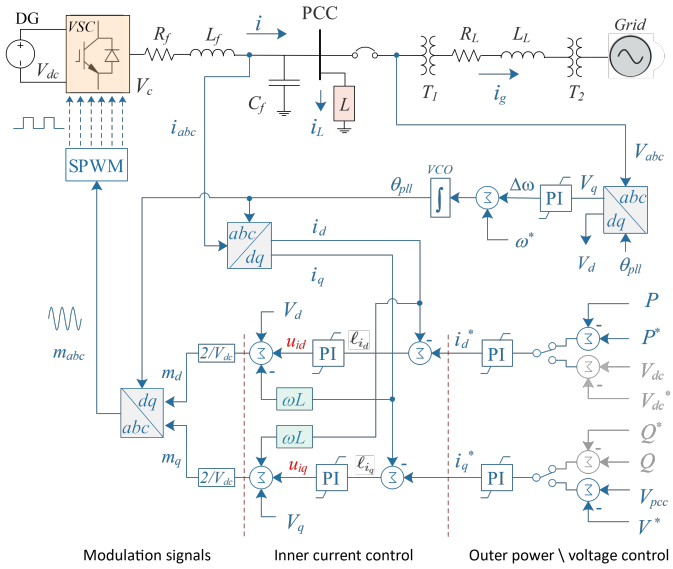

Fig. 1: Schematic control structure of grid-following VSC.

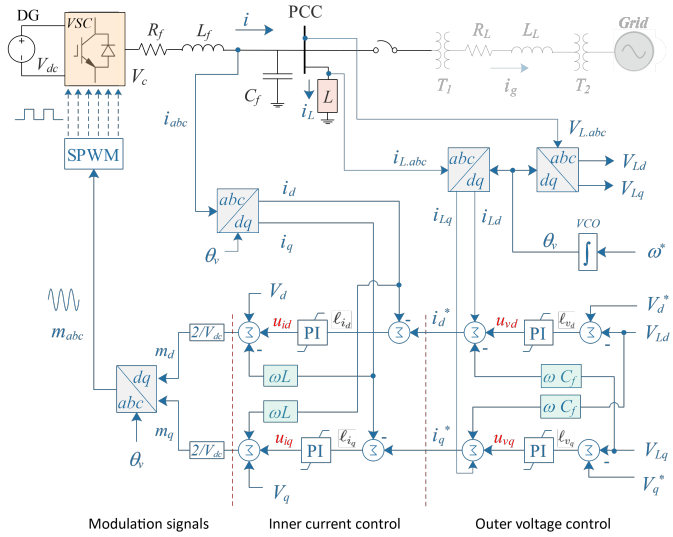

Fig. 2: Schematic control structure of grid-forming VSC.

B. Grid-Forming VSC

A grid-forming VSC can be operated in MGs as the source of voltage and frequency control. Thus, it operates as an ideal ac voltage source with a low output impedance [2].

Fig. 2 presents a schematic diagram of the grid-forming VSC with its control structure in the dq-frame. Part of the control structure is similar to the grid-following control structure except the outer loop. The reference voltages (V_d^*, V_q^*) are to be followed for the outer loop. In addition, instead of relying on the PCC voltage angle for abc/dq frame conversion, the angle is now directly generated by integrating the nominal frequency ω^*. Through this control structure, a grid-forming VSC can regulate voltage and frequency.

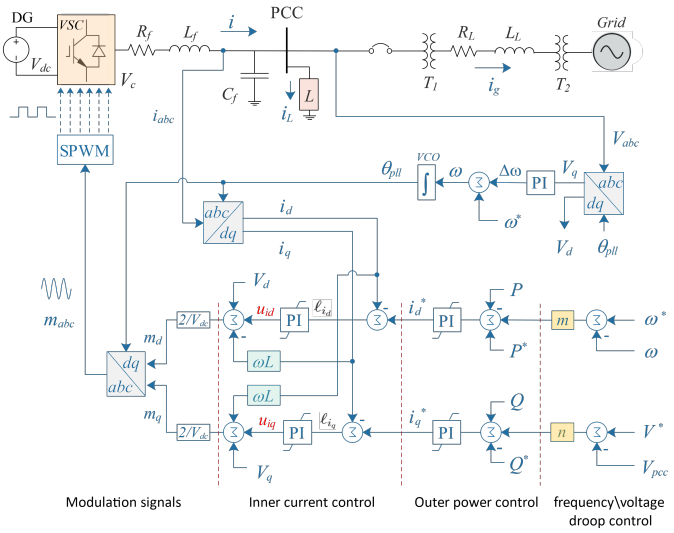

Fig. 3: Schematic control structure of a grid-supporting VSC.

C. Grid-Supporting VSC

A grid-supporting VSC can operate either in grid-connected mode or autonomous mode, with no need to re-configuration of its control. In general, the objectives of a grid-supporting VSC are as follows. a) It can fully supply loads when the MG is isolated from the main grid; b) it can contribute to control the voltage of the MG (PCC voltage) in both modes; c) it can participate controlling the frequency of the MG in both modes; and d) grid-supporting converters can share real and reactive power through their droop design. [2].

The control structure of a three-phase grid-supporting VSC is depicted in Fig. 3. Its control operates as a grid-following VSC with the addition of droop control. The droop control mechanism aims to maintain the voltage and frequency of the grid at their rated values. In the frequency droop loop, the error between the initial ω^* and the measured ω frequency is the input to a droop gain block (m), whose output establishes a droop reference power to P^*. Likewise, the voltage droop is added to the reactive power loop to set up a droop reference power to Q^*. Droop control is widely used in synchronous generators to provide primary frequency control and share load among generators [5]. This control design has now been incorporated into VSCs.

III. VSC Control Design Principles

The PCC voltage oriented vector control has been used in VSC control. This method allows the components of currents and voltages to be converted to DC quantities at steady state in the dq-frame. Therefore, PI controllers can be implemented for precise reference signal tracking [2], [5] , [7].

Subsection ***A*** describes the inner current loops and subsections ***B-D*** show the control structures of the outer loops in each of the VSC controls.

A. Inner Current Control

The three-phase dynamic equation of the VSC system connected to a distribution network is expressed as follow:

$$V_{c_{abc}} - V_{pcc_{abc}} = L_f \frac{\mathrm{d}i_{abc}}{\mathrm{d}t} + R_f i_{abc} \tag{1}$$

where $V_{c_{abc}}$ and i_{abc} are the ac output voltage the current of the converter, respectively, and $V_{pcc_{abc}}$ is the voltage at the PCC.

The current and voltage in (1) are transferred into the dq reference frame by using Park transformer as follows.

$$V_{c_d} - V_{pcc_d} = R_f\, i_d + L_f \frac{\mathrm{d}i_d}{\mathrm{d}t} - \omega L_f\, i_q \tag{2}$$

$$V_{c_q} - V_{pcc_q} = R_f\, i_q + L_f \frac{\mathrm{d}i_q}{\mathrm{d}t} + \omega L_f\, i_d \tag{3}$$

(2) ans (3) are two first order-linear systems where i_d and i_q are coupled by ωL_f. In order to achieve a decouple control of the currents, coupling terms are eliminated by feed-forward signals as shown in Fig. 1. The final voltage in dq-frame is presented in (4) and (5) as:

$$V_{c_d} = u_{id} + V_{pcc_d} - \omega L_f i_q \tag{4}$$

$$V_{c_q} = u_{iq} + V_{pcc_q} + \omega L_f i_d \tag{5}$$

where, $u_{id} = \ell_{i_d}\left(k_{pi} + \frac{k_{ii}}{s}\right)$, $u_{iq} = \ell_{i_q}\left(k_{pi} + \frac{k_{ii}}{s}\right)$, and ℓ_{i_d}, ℓ_{i_q} are the errors between the reference and measurement currents in dq-frame.

V_{c_d} and V_{c_q} are linearly proportional to the modulation signals m_d and m_q, respectively, by a proportionality gain of $V_{dc}/2$. Finally, the VSC current controllers are limited to protect the converter against overcurrents [7], [9].

B. Grid-Following: Power & Voltage Control

In the case of grid-following converters, the reference currents i_d^* and i_q^* are commonly provided by a power controller in which it controls the powers delivered to the grid and the local load. Powers components are expressed as follow.

$$P = V_{pcc_d}\, i_d \quad , \quad Q = -V_{pcc_d}\, i_q \tag{6}$$

Thus, the outer loop of the active power regulates the power P at its reference value P^* and generates the d-axis current reference signal i_d^* for the inner current control. Either the reactive power Q or the PCC voltage V_{pcc} is adjusted through i_q^* as illustrated in Fig. 1.

Note also due to the relationship in (6), the real power control assumes negative feedback control while the reactive power or ac voltage control assumes a positive feedback control. In case the dc-link voltage is to be regulated, positive feedback control is employed since the dc-link voltage decreases if the real power export increases.

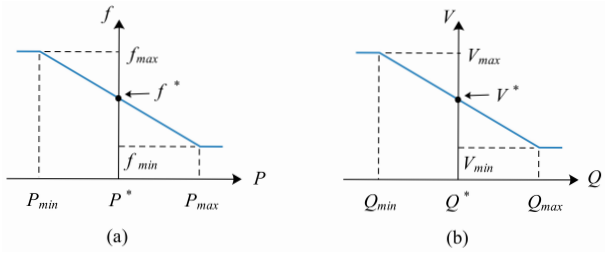

Fig. 4: Conventional droop characteristics: (a) *P-f* droop (b) *Q-V* droop.

C. Grid-Forming: Voltage Control

A grid-forming VSC consists of two cascaded loops, as shown in Fig. 2. The external voltage loop provides the current reference i_d^* and i_q^* to the inner current loop, to be injected by the converter. The dynamic equation of the voltage controller is expressed in the dq-frame as follows.

$$C_f \frac{\mathrm{d}}{\mathrm{d}t} V_{L_d} = i_d - i_{L_d} + \omega C_f\, V_{L_q} \tag{7}$$

$$C_f \frac{\mathrm{d}}{\mathrm{d}t} V_{L_q} = i_q - i_{L_q} - \omega C_f\, V_{L_d} \tag{8}$$

where V_L and i_L are the voltage and current of the load.

Decoupling feed-forward compensations are implemented to the control system in order to eliminate the coupling terms between V_{Ld} and V_{Lq}. Consequently, the load voltage V_{Ld} and V_{Lq} can be controlled by i_d^* and i_q^*, respectively. The dq reference currents are determined as:

$$i_d^* = u_{vd} + i_{L_d} - \omega\, C_f\, V_{L_q} \tag{9}$$

$$i_q^* = u_{vq} + i_{L_q} + \omega\, C_f\, V_{L_d} \tag{10}$$

where, $u_{vd} = \ell_{v_d}\left(k_{pd} + \frac{k_{id}}{s}\right)$, $u_{vq} = \ell_{v_q}\left(k_{pq} + \frac{k_{iq}}{s}\right)$, and ℓ_{v_d}, ℓ_{v_q} are the errors between the reference and measurement voltages of the load in dq-frame.

D. Grid-Supporting: Droop Control

In grid-supporting VSCs, the droop controls are implemented on top of a grid-following control structure, as shown Fig. 3. The droop controls permit regulating the MG frequency and voltage at the PCC by controlling the proper active and reactive power delivered to the grid and the load. The droop control expressions are as follows.

$$f - f^* = -\,m\,(P - P^*) \tag{11}$$

$$V - V^* = -\,n\,(Q - Q^*) \tag{12}$$

where $(V - V^*)$ and $(f - f^*)$ is the PCC voltage and frequency deviations from their nominal values, respectively. The variation in powers $(P - P^*)$ and $(Q - Q^*)$ is to be compensated by the VSC system. The gain droop parameters m and n represent the slope of the frequency and voltage droops. Fig. 4 presents the graphically relationships of the droop characteristics.

Table I: The testbeds parameters

	Description		Parameters	Value
Grid side	Transformer 1		T_1	400 kVA 260 V \ 25 kV
	Transformer 2		T_2	400 kVA 25 kV \ 120 kV
	Transmission line		R_L , X_L	0.1X_L , *0.2 pu*
DG side	Rated power		S_b	400 kW
	Rated voltage		*ac/dc side*	260/500 V
	Converter filter		R_f	0.156/50 pu
			X_f	0.156 pu
	Shunt capacitor		C_f	0.25 pu
	dc power source		V_{dc}	500 V
VSC Control	Grid-Following & Supporting Outer loops	power loop	K_{pp} , K_{ip}	1 , 100
		voltage loop	K_{pv} , K_{iv}	1 , 400
		Droop control	m	0.526
	Grid-Forming Outer loops	*dq*-axis voltage loops	K_{pd} , K_{id}	1 , 100
			K_{pq} , K_{iq}	1 , 100
	Inner current control		K_{pi} , K_{ii}	0.3 , 5
	PLL		$K_{p,PLL}$, $K_{i,PLL}$	60 , 1400

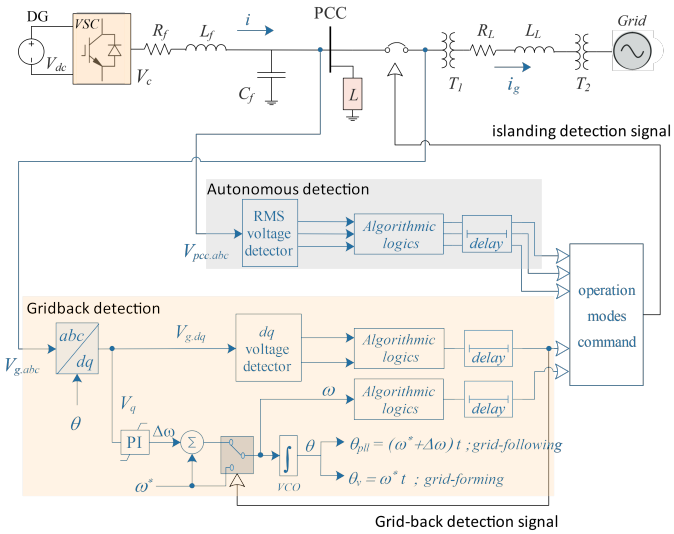

Fig. 5: Detection schemes for operation in both grid-connected and islanded modes.

IV. EMT TESTBEDS DESCRIPTION

A. System Description

The simulated system is composed of a single DER represented by a dc voltage source at 500 V, an interfacing two-level VSC, an RL filter, shunt compensation, and a local load (series RL) connected at the PCC. The VSC system is connected to a grid through a main switch. Thus it can operate in either the grid-connected or the autonomous modes. The converter is connected to a 120 kV grid through two step up transformers and an 25 kV line. The shunt compensation is assumed at 25% of the system rated power. The system parameters are given in Table I.

B. Detections Scheme for Islanding and Synchronization

A management control system of MGs is necessary to monitor the condition of the network and its mode of operation. A detection scheme in a MG has the ability to detect a network disturbance and then to isolate the MG from the grid by opening the main switch. Islanding detection strategies have been proposed in [7], [10]. The passive method is one most commonly adopted islanding detection method. It depends on measuring system parameters to detect autonomous or grid-connected operation.

Fig. 5 shows the basic detection control scheme based on the Over/Under voltage protection (OVP/UVP) and the Over/Under frequency protection (OFP/UFP) where its upper-lower limit thresholds are selected 95%-105% for the voltage and 59.3-60.5 Hz for the frequency. Two detection circuits are implemented: Autonomous and Gridback detection schemes. The autonomous detection scheme is based on the PCC voltage and it is responsible to detect the islanding mode. The Gridback detection scheme depends on monitoring the grid voltage and it aims to re-synchronize the VSC to the grid before the main switch is closed. In one testbed, the VSC control is required to switch from grid-forming to grid-following. The detectors of the voltages can be either in abc or dq frames.

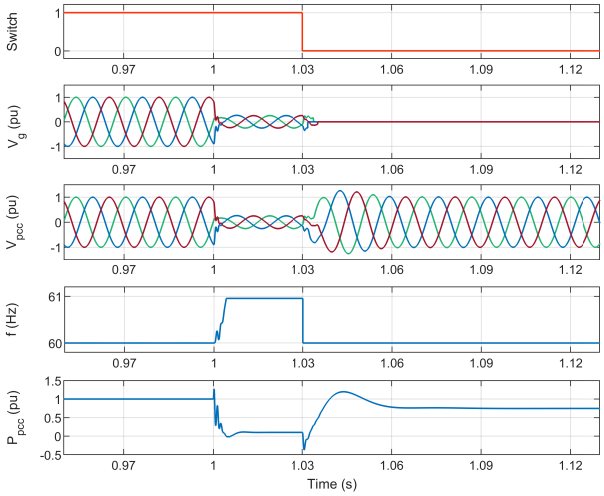

Fig. 6: Responses during the switching process of the VSC system from grid-connected mode (grid-following) to autonomous mode (grid-forming) due to an accidental condition.

V. CASE STUDIES & SIMULATION RESULTS

To compare the effectiveness of the three control techniques of the VSC system, two testbeds are setup in MATLAB/SimPowerSystems. They are described as follows. In Testbed 1, the VSC control is implemented as grid-following parallel with an inactive grid-forming during grid-connected mode. Until it receives a signal from the autonomous detection scheme, the VSC control switches control. In Testbed 2, grid-supporting VSC is adopted regardless of islanding or synchronization. In each tesbed, simulation results will present two events: islanding and re-synchronizing. For faster simulation speed, average model for the converter is adopted.

A. Testbed 1: Grid-Following & Grid-Forming VSC

During the grid-connected operation, the VSC control is implemented as grid-following VSC, as shown in Fig. 1, where the active power and the PCC voltage are to be controlled. The inactive grid-forming control, as depicted in Fig. 2, is in parallel with the grid-following control and it will be activated when the MG is commanded to operate in the autonomous mode, where the voltage and frequency of the MG are regulated.

Initially, the MG operates in the gird-connected operation mode when the main switch is closed. It is commanded to supply a total active power of $P^* = 1\ pu$, and meanwhile to regulate the PCC voltage at its rated voltage ($V^* = 260\ V$). The power produced by the VSC (P_{pcc}) is delivered to a load that absorbs a fixed active power of $0.75\ pu$ in both modes of operation and the rest of the power is transferred to the grid ($P_g = 0.25\ pu$).

A three-phase fault occurs on the AC system at $t = 1\ s$ while the main switch still closes at the moment. However, the control configuration of the VSC system remains operated in the grid-following under that condition. It can be seen in Fig. 6 that $V_{pcc.abc}$ and $V_{g.abc}$ are reduced during the fault condition and before the main switch is opened. Also, the frequency w sensed by the PLL increases to its upper limits of 383 rad/s due to the imposed limitation of the PI controller in the PLL.

When the accidental islanding condition is detected in 30 ms, the main switch is opened by changing the operation modes command from 1 to 0. Thus, the control of the VSC is switched to the grid-forming where the frequency ω is set to $\omega^* = 377\ rad/s$. Furthermore, the load voltage V_L is regulated at its nominal value whereas the grid voltage becomes zero. Therefore, the VSC system is able to deliver an active power of $P_{pcc} = 0.75\ pu$ to the load. The system response of the switching command signal, V_{gabc}, $V_{pcc.abc}$, system frequency, and the active power through the PCC are presented in Fig. 6.

When the fault is cleared at $t = 5\ s$, and the grid returns to its normal operation, the MG is supposed to operate its converter back to the grid-following where the frequency is imposed by the grid. The voltage V_{pcc} is required to be re-synchronized to the grid voltage V_g before closing the main switch in order to have a smooth transient that may occur due to the switching of the operation mode. V_{gq} is assumed to be a negative and large value due to the phase shift, $V_{pcc.a}$ lags $V_{g.a}$ by 90°, as shown in Fig. 8. After an intentional delay of 0.04 s, the frequency mode of the VCO is switched by the gridback mode signal, at $t = 5.04\,s$, as shown in Fig. 7, from the grid-forming, in which $\theta_v = \omega^* t$, to the grid-following, in which it depends on the output of the PLL controller, that is, $\theta_{pll} = (\omega^* + \Delta\omega)t$. Thus, the PLL starts to sense the grid voltage, and then it drops to its lower limit of 371 rad/s due to the PLL controller reduces ω to adjust V_{gq} at zero. When ω reaches its nominal value, the V_{gq} and the phase shift tend to approach zero. Once the PLL reaches its steady state, the

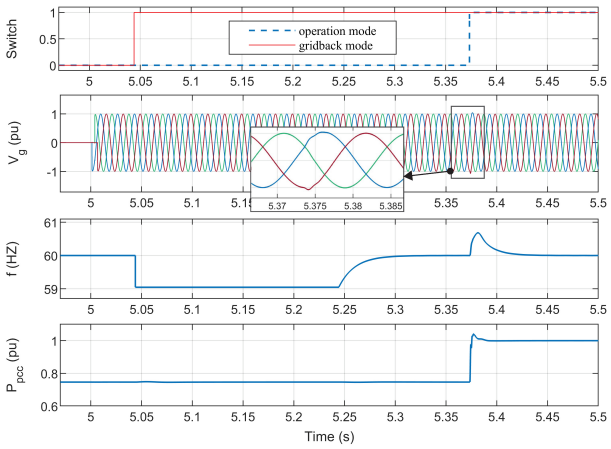

Fig. 7: Responses during the switching process of the VSC system from autonomous mode (grid-forming) to grid-connected mode (grid-following) when the fault is cleared.

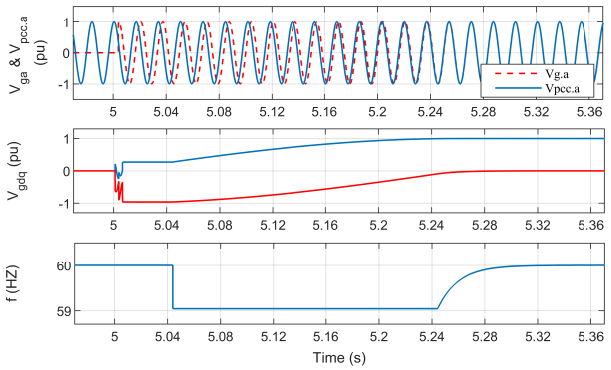

Fig. 8: A closer look of the system responses during the synchronization process: phases a for both grid voltage and PCC voltage, grid voltage in dq, and PLL frequency.

main switch is commanded to close, at $t = 5.375\ s$, by the signal of the operation mode. Now, the MG is operated in the grid-following VSC. In Fig. 7, the active power P_{pcc} is returned to its rated value ($P^* = 1\ pu$).

B. Tesbed 2: Grid-Supporting VSC

This testbed shows the switching process from one to another mode of the MG operation where grid-supporting VSC is adopted, as depicted in Fig. 3.

Fig. 9 describes the system responses during the switching to autonomous mode due to a fault condition. The autonomous mode is detected in 30 ms, thus the MG is isolated from the grid. The MG frequency has a new stable operating point with a deviation due to the variation in power. Initially, the active power reference P^* is set to 1 pu before the operation mode is changed. Thus, the active power regulated by the VSC decreases a $0.25\ pu$ of the initial value in order to feed the load ($P_L = 0.75\ pu$). The frequency deviation can be determined as ($\Delta\omega = \frac{\Delta P}{m} = 0.475\,Hz$) [5]. It is worth to mention

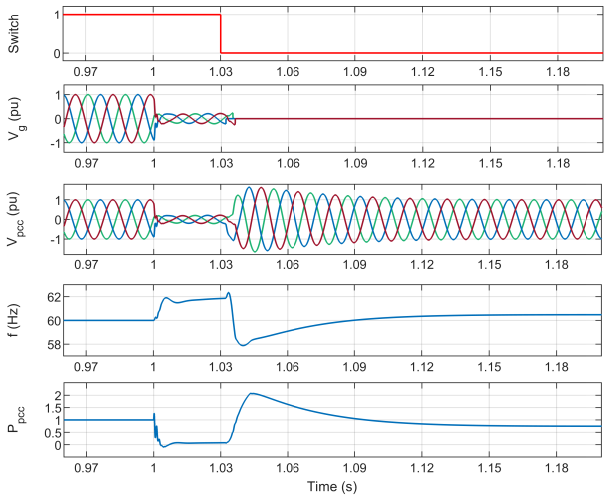

Fig. 9: Response system of switching behavior to the autonomous mode in the grid-supporting VSC.

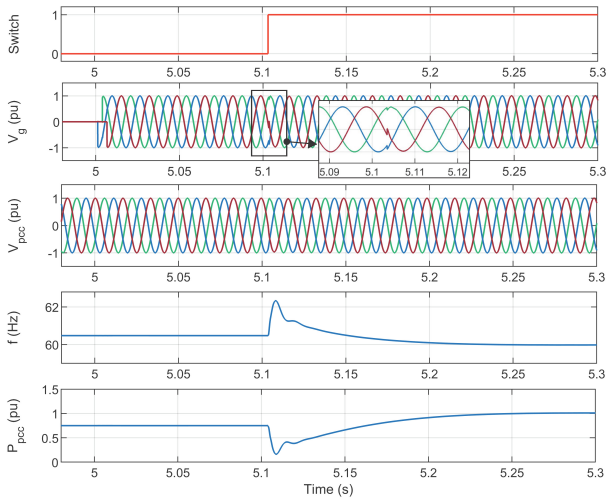

Fig. 10: Response system of switching behavior to the grid-connected mode in the grid-supporting VSC.

that the PLL is not limited in this case, thus the frequency droop control is be able to limit the frequency during the fault condition.

When the grid returns to its normal operation, the MG may be re-switched to the grid-connected mode after the fault is cleared at $t = 5\ s$. The mode of operation is commanded to switch after a delay of about $0.11\ s$ from the fault clearance as shown in Fig. 10. Since the system frequency in both modes is regulated by the PLL, it is able to synchronize the PCC voltage to the grid voltage. Due to the phase shift between the PCC voltage and grid voltage, $V_{pcc.a}$ leads $V_{g.a}$ by $90°$, as shown in Fig. 11, in which resulting in an overshoot in the frequency. It can be seen that the active power regulated by the VSC system P_{pcc} returns to its reference value in which the VSC system delivers 0.25 % and 0.75 % of its output power to the grid and the load, respectively.

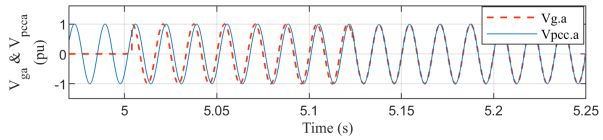

Fig. 11: A closer look of the phase shift of phase a between the PCC voltage V_{pcc} (converter side) and the grid voltage V_g (grid side).

VI. Conclusion

In this paper, first, an overview of three different control mechanisms of a VSC operated in a MG are presented and discussed: grid-following, grid-forming, and grid-supporting. Their control configurations are classified based on their VSC's role in MG operation. Secondly, comparison of theses control techniques is provided using two tesbeds built in MATLAB/SimPowerSystem environment. The simulation results of switching from one operation to another operation, namely, islanding and re-synchronization, are examined. Compared to either the grid-following or grid-forming VSCs, grid-supporting VSC has the advantage of operating in the both operation modes without changing control configuration. The droop control has been identified as an effective tool to participate in regulating the frequency of the grid.

References

[1] G. Pepermans, J. Driesen, D. Haeseldonckx, R. Belmans, and W. Dhaeseleer, "Distributed generation: definition, benefits and issues," *Energy policy*, vol. 33, no. 6, pp. 787–798, 2005.

[2] J. Rocabert, A. Luna, F. Blaabjerg, and P. Rodriguez, "Control of power converters in ac microgrids," *IEEE transactions on power electronics*, vol. 27, no. 11, pp. 4734–4749, 2012.

[3] M. Liserre, A. Pigazo, A. Dell'Aquila, and V. M. Moreno, "An anti-islanding method for single-phase inverters based on a grid voltage sensorless control," *IEEE Transactions on Industrial Electronics*, vol. 53, no. 5, pp. 1418–1426, 2006.

[4] J. M. Carrasco, L. García Franquelo, J. T. Bialasiewicz, E. Galván, R. C. Portillo Guisado, M. d. l. Á. Martín Prats, J. I. León, and N. Moreno-Alfonso, "Power-electronic systems for the grid integration of renewable energy sources: A survey," *IEEE Transactions on Industrial Electronics, 53 (4), 1002-1016.*, 2006.

[5] L. Fan, *Control and dynamics in power systems and microgrids*. CRC Press, 2017.

[6] B. Kroposki, B. Johnson, Y. Zhang, V. Gevorgian, P. Denholm, B.-M. Hodge, and B. Hannegan, "Achieving a 100% renewable grid: Operating electric power systems with extremely high levels of variable renewable energy," *IEEE Power and Energy Magazine*, vol. 15, no. 2, pp. 61–73, 2017.

[7] A. Yazdani and R. Iravani, *Voltage-sourced converters in power systems: modeling, control, and applications*. John Wiley & Sons, 2010.

[8] F. Blaabjerg, R. Teodorescu, M. Liserre, and A. V. Timbus, "Overview of control and grid synchronization for distributed power generation systems," *IEEE Transactions on industrial electronics*, vol. 53, no. 5, pp. 1398–1409, 2006.

[9] N. Mohan, T. M. Undeland, and W. P. Robbins, *Power electronics: converters, applications, and design*. John wiley & sons, 2003.

[10] S.-I. Jang and K.-H. Kim, "An islanding detection method for distributed generations using voltage unbalance and total harmonic distortion of current," *IEEE transactions on power delivery*, vol. 19, no. 2, pp. 745–752, 2004.